Mountain torques and atmospheric oscillations

François Lott

Laboratoire de Météorologie Dynamique, Université Pierre et Marie Curie, Paris, France

Andrew W. Robertson and Michael Ghil

Department of Atmospheric Sciences and IGPP, University of California at Los Angeles, USA

Abstract. Theoretical work and general circulation model (GCM) experiments suggest that the midlatitude jet stream's interaction with large-scale topography can drive intraseasonal oscillations in large-scale atmospheric circulation patterns. In support of this theory, we present new observational evidence that mountain-induced torques play a key role in 15–30-day oscillations of the Northern Hemisphere circulation's dominant patterns. The affected patterns include the Arctic Oscillation (AO) and the Pacific–North-American (PNA) pattern. Positive torques both accelerate and anticipate the midlatitude westerly winds at these periodicities. Moreover, torque anomalies anticipate the onsets of weather regimes over the Pacific, as well as the break-ups of hemispheric-scale regimes.

Introduction

Observational studies show that, above a broad-band background, midlatitude low-frequency variability (LFV) is characterized by intermittent weather regimes [*Cheng and Wallace*, 1993; *Kimoto and Ghil*, 1993], and by intraseasonal oscillations [*Branstator*, 1987; *Kushnir*, 1987; *Ghil et al.*, 1991]. The latter are known to be modulated by tropical convection at the 30–60-day time scale of the Madden–Julian Oscillation (MJO) [*Madden and Julian*, 1994; *Higgins and Mo*, 1997], and the 2–6-year time scale of the El Niño–Southern Oscillation (ENSO) [*Rasmusson and Mo*, 1993]. On the other hand, theoretical model studies [*Charney and DeVore*, 1979; *Pedlosky*, 1981; *Legras and Ghil*, 1985; *Jin and Ghil*, 1990] suggest that the midlatitude jet stream's interaction with large-scale topography can drive midlatitude intraseasonal oscillations in both zonal and non-zonal winds.

This theory of oscillatory topographic instability is supported by numerical experiments using quasi-geostrophic models with full-sphere geometry and realistic topography [*Strong et al.*, 1995] as well as by GCM simulations [*Marcus et al.*, 1996]. *Ghil and Robertson* [2000] discuss the topographically driven oscillations' properties across a full hierarchy of models. So far, direct observational support for oscillatory topographic instability has been fairly limited [*Metz*, 1985]. The theory, if correct, implies that mountain torques drive a significant fraction of atmospheric variability within an intraseasonal frequency band and might have predictive value.

The link between mountain torques and changes in global atmospheric angular momentum M is well established [*Hide et al.*, 1980; *Hide and Dickey*, 1991]. Changes in M arise either through torques exerted at the lower boundary by small-scale turbulent friction or by surface-pressure differences across mountains. On time scales shorter than a season, the relative role of these two factors in affecting M is subject to debate. In the 30–60-day band, M-changes are driven about equally by the mountain torque T_M and by frictional torque T_F; changes in T_F accompany the MJO through tropical surface-wind anomalies [*Madden*, 1987; *Madden and Speth*, 1995; *Weickmann et al.*, 1997]. At periodicities below 15 days, M-changes are primarily related to mountain torque changes that accompany synoptic weather systems as they cross the Rockies or the Himalayas [*Iskenderian and Salstein*, 1998].

The intermediate 15–30-day band, however, where major extratropical oscillations occur [*Branstator,* 1987; *Kushnir,* 1987; *Ghil and Robertson,* 2000, and further references therein], has not been examined in sufficient detail. This is surprising, since in the Northern Hemisphere (NH), significant cross-spectral peaks between T_M and barotropic zonal wind occur at periods above 15 days, while T_M also affects a blocking index at these time scales [*Metz*, 1985]. Using a much longer and physically more self-consistent dataset than was available to *Metz* in 1985, we demonstrate that (i) the 15–30-day band is precisely the one where the mountain torque exhibits its most significant spectral peaks; (ii) these spectral peaks in T_M are linked to large-scale atmospheric flow patterns; and (iii) changes in T_M anticipate those in the flow patterns.

Results

The 40-year NCEP/NCAR reanalysis dataset [*Kalnay et al.*, 1996] is ideal for our purpose. It is a dynamically complete set of meteorological fields for 1958–1997, constructed with NCEP's current data assimilation system. To assess its accuracy we have computed the global angular momentum budget for 1958–1997 and verified that the tendency dM/dt is very similar to the independent estimate of *Madden and Speth* [1995], based on ECMWF data. In addition, the total torque $T_M + T_F$ does follow dM/dt very closely (cf. Appendix A). Over the full 40-year, the correlation coefficient r between dM/dt and the total torque is $r = 0.87$.

Our results are presented for the NH, north of 20^oN. The power spectrum of NH mountain torque (Figure 1), constructed using the multi-taper method (MTM see Appendix B) [*Thomson*, 1982; *Dettinger et al.*, 1995; *Mann and Lees*, 1996], exhibits five significant peaks in the 15–30-day range above an almost white background. The MTM spectrum drops sharply for periods longer than 30 days, indicating

Paper number 2000GL011048.
0094-8276/01/2000GL011048$05.00

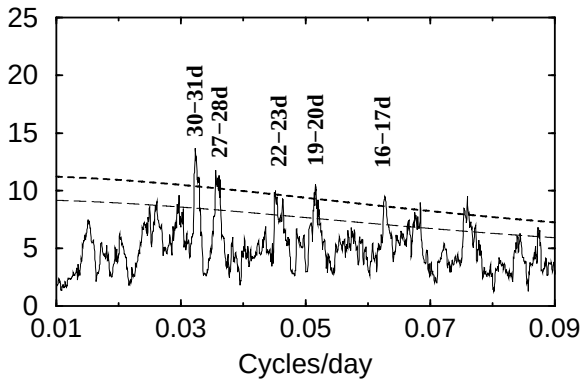

Figure 1. MTM spectra of NH T_M based on time series of 3-day averages, using 8 tapers and a resolution of 1.3710^{-3}cy/day. The light (heavy) dashed line gives the 95% (99%) significance level.

that the MJO cannot affect the NH mountain torque in a major way.

To capture the dominant spatial patterns of atmospheric flow variability, we take 3-day-mean geopotential height maps of the 700-hPa pressure surface and compute empirical orthogonal functions (EOFs) over the NH, as well as over the Pacific-North-American (*PAC*) sector (120^oE-60^oW, 20^oN-90^oN). The first two NH EOFs have a large zonally symmetric component. The first EOF (Figure 2a) describes changes in the midlatitude zonal-wind speed and mass distribution that are associated primarily with the subtropical jet and the seasonal cycle. The second NH EOF (Figure 2b) describes modulations in the strength of the polar vortex and resembles the lower-tropospheric manifestation of the AO [*Thomson and Wallace*, 1998]. The third *PAC* EOF (Figure 2c) corresponds to an east-west dipole centered over the Rockies that resembles the PNA pattern [*Wallace and Gutzler*, 1981]; its primary center of action, over the northeastern Pacific, describes an anomalous extension or contraction of the jet stream in this sector.

We project the individual 700-hPa height maps onto the three EOFs in Figure 2 to obtain the corresponding principal components (PCs). Each of their spectra (not shown) exhibits significant peaks in the 15–30-day band. To quantify the correspondence between these peaks and those in the NH T_M (Figure 1), we focus on the 15–30-day range by band-pass filtering all series between 15 and 35 days (see Appendix B). The amplitudes of the four resulting series (for the torque and the three PCs respectively) are quite substantial: after subtracting the seasonal cycles they account for typically 25% of the variance of the respective unfiltered time series. The NH T_M and the PCs show highly significant lag correlations in all three cases (Figure 3). The correlations between the unfiltered time series with the seasonal cycle removed (not shown) are about half as large as in the filtered data.

For NH PCs 1 and 2, the correlations are nearly antisymmetric with respect to lag, and near-zero at zero lag. This phase quadrature agrees with the dominance of T_M in Eq. (1) for our intraseasonal frequency band. Positive values of T_M, i.e. an eastward acceleration of the atmosphere, *lead* positive coefficients of NH EOFs 1 and 2. Thus stronger than usual midlatitude westerly winds follow larger T_M by up to about 10 days. To corroborate that these 15–30-day variations in NH T_M are a key driver of midlatitude changes in M, we integrated dM/dt between 20^oN and 90^oN over the 15–30-day band. The angular momentum tendency's variations are very close in amplitude and phase to those in NH mountain torque; their correlation at zero lag is $r = 0.7$.

The surface pressure changes associated with the hemispheric EOFs 1 and 2 are essentially meridional (Figures 2a,b), while the patterns that produce a large T_M exhibit strong zonal gradients of surface pressure and 700-hPa geopotential height across the Rockies and Himalayas respectively (not shown). Hence a strong mountain torque signal cannot be a passive by-product of the flow changes associated with PCs 1 and 2. This observation is entirely consistent with the correlations between T_M on the one hand, and PCs 1 and 2, on the other, being almost zero at zero lag (Figure 3).

The Pacific sectorial PC-3's correlation with the mountain torque is also highly significant and shows the torque to lead the PC. Thus, mountain forcing anticipates changes in the dominant pattern of Pacific-sector variability (Figure 2c). These changes, in turn, affect the intensity of the jet over the northeastern Pacific and thus the angular momentum M. In contrast to the hemispheric PCs, the third Pacific EOF is itself associated with a large pressure difference across the Rockies and, therefore, a mountain torque. This is consistent with the smaller phase lag between the torque and *PAC* PC-3, compared to the hemispheric modes (Figure 3).

To check the potential significance of our findings for extended-range prediction, we have isolated the dominant patterns of atmospheric LFV using an analysis of weather regimes [*Ghil et al.*, 1991]. Our analysis reproduces the NH and *PAC* regimes found in previous studies during the winter months [*Kimoto and Ghil*, 1993; *Cheng and Wallace*, 1993; *Smyth et al.*, 1999]. The first and third hemispheric regimes, by frequency-of-occurrence, resemble contrasting phases of the AO, i.e. of NH EOF 2 (Figure 2b). NH mountain torque variations in the 15–30-day band contribute to the break-up of both of these regimes. Over the *PAC* sector, we find that unfiltered torque anomalies anticipate the onset of the two most significant Pacific regimes – which resemble opposite polarities of *PAC* EOF 3 – by a few days.

Summary

Our observational results indicate that large-scale changes in the extratropical atmosphere with periods of 15–30 days are often anticipated by mountain–torque changes. For the NH EOFs 1 and 2 we find strong evidence that the mountain torque actively drives these changes because: (i) the torque leads the PCs in phase quadrature; and (ii) both EOFs patterns are zonally symmetric to a large degree and thus very different from flow patterns that would produce a large mountain torque *per se*. For the Pacific-sector EOF 3, we find T_M to lead its PC by about $\pi/3$. This phase relationship is consistent with *PAC* PC 3 being associated with changes in the jet intensity over the northeastern Pacific and thus atmospheric angular momentum M.

The changes induced by the torque affect the onset and break of important patterns of NH LFV, in particular the AO and the PNA pattern. These observational findings are entirely consistent with the theory of oscillatory topographic instability [*Legras and Ghil*, 1985; *Jin and Ghil*, 1990]. The

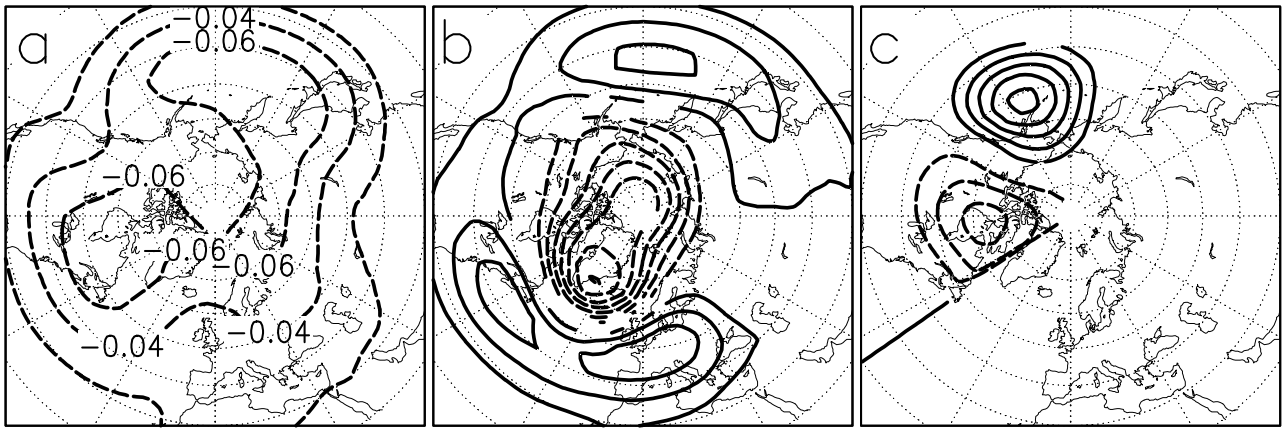

Figure 2. EOFs of 700-hPa geopotential heights evaluated over 1958–1997 using maps of three-day means. a) EOF 1 for NH; b) EOF 2 for NH; and c) EOF 3 for *PAC*. Negative contours are dashed.

theory's predictions have been verified now across a full hierarchy of models [*Strong et al.*, 1995; *Marcus et al.*, 1996; *Ghil and Robertson*, 2000] and provide the most plausible mechanism so far to explain our observational findings.

Appendix A: Angular momentum budget

The budget of angular momentum M is given by

$$\frac{dM}{dt} = T_M + T_F \quad , \tag{A1}$$

where T_M is the mountain torque and T_F is the friction torque (see for instance [*Madden and Speth*, 1995]). Daily zonal-wind averages u, at the 19 reanalysis pressure (p) levels, together with daily averages of surface pressure p_s, were used to compute M. T_M consists of an explicit pressure term which involves the zonal gradient of the mountain height h and a gravity-wave stress τ_G. The latter and the boundary-layer stress τ_B needed for T_F are estimated using their parameterized values taken from NCEP's 6-hour forecasts. Gravity-wave stresses are difficult to estimate accurately [*Lott and Miller*, 1997]. They were found to degrade the angular momentum balance and were therefore excluded from our calculations. We analyze three-day averages of all quantities and focus on T_M evaluated using only pressure and topographic height, both of which are directly measured quantities. The 40-year grand mean was subtracted to eliminate systematic biases due to inaccuracies in the parameterized values of τ_G and τ_B.

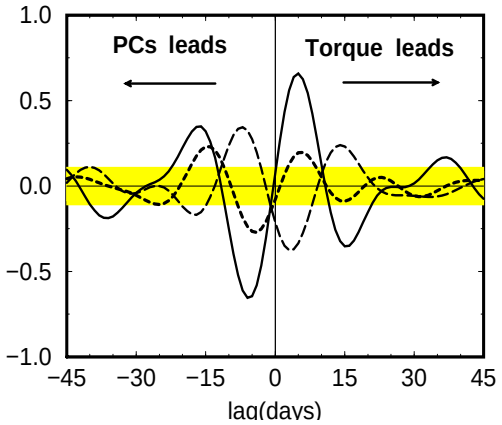

Figure 3. Lag correlations between the NH T_M and the PCs in the 15–30-day band. Solid curve: NH PC-1; short dashed curve: NH PC-2; long dashed curve *PAC* PC-3. Shaded: 99% confidence interval from a Monte Carlo test using correlations at random lags.

Appendix B: Spectral analysis methods

All spectral analyses shown in Figure 1 and mentioned in the text were performed using the SSA-MTM Toolkit [*Dettinger et al.*, 1995]; its latest version, Version 4.0, is available as freeware at http://www.atmos.ucla.edu/tcd/.

The band-pass filter used in Figure 3 and elsewhere in the text is based on a Kaiser window and its parameters are adjusted to minimize Gibbs effects [*Hamming*, 1983; *Scavuzzo et al.*, 1998]. The resulting transfer function is very close to unity for 16–30 days and nearly zero above 44 and below 13 days; its half-power points are at 15 and 35 days.

Acknowledgments. The authors are grateful to associates on three continents for interesting exchanges on low-frequency atmospheric variability. Comments from J. O. Dickey, K. Ide, R. A. Madden, S. L. Marcus, W. Metz, H. L. Swinney, Y. Tian, K. M. Weickmann and an anonymous reviewer helped improve the presentation. The NCEP/NCAR Reanalysis data are provided through the NOAA Climate Diagnostics Center (http ://www.cdc.noaa.gov). This work was supported by NASA's Global Modeling and Analysis Program (F.L.), DOE's Office of Biological and Environmental Research (A.W.R.), and an NSF Special Creativity Award (M.G.). This is publication no. 5496 of UCLA's IGPP.

References

Branstator, G. W., A striking example of the atmosphere's leading traveling pattern, *J. Atmos. Sci., 44,* 2310-2323, 1987.

Charney, J. G. and J. G. DeVore, Multiple flow equilibria in the atmosphere and blocking, *J. Atmos. Sci., 36,* 1205-1216, 1979.

Cheng, X. and J. M. Wallace, Cluster analysis of the northern hemisphere wintertime 500-hPa height field: spatial patterns, *J. Atmos. Sci., 50,* 2674-2696, 1993.

Dettinger, M. D., Strong, C. M., Weibel, W., Ghil, M. and P. You, Software for singular spectrum analysis of noisy time series, *Eos Trans. AGU 76(2),* 12-14-21, 1995.

Ghil, M., Kimoto, M. and J. D. Neelin, Nonlinear dynamics and predictability in the atmospheric sciences, *Rev. Geophys. Suppl., 29*, 46-55, 1991.

Ghil, M., and A. W. Robertson, Solving problems with GCMs: General circulation models and their role in the climate modeling hierarchy. In *General Circulation Model Development: Past, Present and Future,* Edited by D. Randall, pp. 285-325, Academic Press, San Diego, 2000.

Hamming, R. W. *Digital Filters,* Chapters 7 & 9, Prentice-Hall, 1983.

Hide, R. and J.O. Dickey, Earth's variable rotation, *Science, 253*, 629-637, 1991.

Hide, R., Birch, N. T., Morrison, L. V., Shea, D. J. and A. A. White, Atmospheric angular momentum fluctuations and changes in the length of day, *Nature, 286,* 114-117, 1980.

Higgins, R. W. and K. G. Mo, Persistent North Pacific circulation anomalies and the tropical intraseasonal oscillation, *J. Climate, 10,* 223-244, 1997.

Iskenderian, H. and D. A. Salstein, Regional sources of mountain torque variability and high frequency fluctuations in atmospheric angular momentum, *Mon. Wea. Rev., 126,* 1681-1694, 1998.

Jin, F.-F. and M. Ghil, Intraseasonal oscillations in the extratropics: Hopf bifurcation and topographic instabilities, *J. Atmos. Sci., 47,* 3007-3022, 1990.

Kalnay E., M. Kanamitsu, R. Kistler, W. Collins, D. Deaven, L. Gandin, M. Iredell, S. Saha, G. White, J. Woollen, Y. Zhu, M, Chelliah, W. Ebsuzaki, W. Higgins, J. Janowiak, K. C. Mo, C. Ropelewski, J. Wang, A. Leetma, R. Reynolds, R. Jenne and D. Joseph, The NCEP/NCAR 40-year reanalysis project, *Bull. Amer. Meteor. Soc., 77,* 437-470, 1996.

Kimoto, M. and M. Ghil, Multiple flow regimes in the Northern Hemisphere winter, *J. Atmos. Sci., 50,* 2625-2673, 1993.

Kushnir, Y., Retrograding wintertime low-frequency disturbances over the North Pacific Ocean, *J. Atmos. Sci., 44,* 2727-2742, 1987.

Legras, B. and M. Ghil, Persistent anomalies, blocking and variations in atmospheric predictability, *J. Atmos. Sci., 42,* 433-471, 1985.

Lott, F. and M. J. Miller, A new subgrid-scale orographic drag parameterization: Its formulation and testing, *Q. J. R. Meteorol. Soc., 123,* 101-127, 1997.

Madden, R. A., Relationships between changes in the length of day and the 40 to 50 day oscillation in the tropics, *J. Geophys. Res., 92,* 8391-8399, 1987.

Madden, R. A. and P. R. Julian, Observations of the 40-50 day tropical oscillation-A review, *Mon. Wea. Rev., 122,* 814-837, 1994.

Madden, R. A. and P. Speth, Estimates of atmospheric angular momentum, friction, and mountain torques during 1987-88, *J. Atmos. Sci., 52,* 3681-3694, 1995.

Mann, M. E. and J. M. Lees, Robust estimation of background noise and signal detection in climatic time series, *Climate Change, 33,* 409-445, 1996.

Marcus, S. L., Ghil, M. and J. O. Dickey, The extratropical 40-day oscillation in the UCLA general circulation model. Part II: Spatial structure. *J. Atmos. Sci., 53,* 1993-2014, 1996.

Metz, W., Wintertime blocking and mountain forcing of the zonally averaged flow: a cross-spectral time series analysis of observed data, *J. Atmos. Sci., 42,* 1880-1892, 1985.

Pedlosky, J., Resonant topographic waves in barotropic and baroclinic flows, *J. Atmos. Sci., 38,* 2626-2641, 1981.

Rasmusson, E. M. and K. C. Mo, Linkages between 200 mb tropical and extratropical circulation anomalies during the 1986-1989 ENSO cycle, *J. Climate, 6,* 595-616, 1993.

Scavuzzo, C. M., Lamfri, M. A., Teitelbaum, H. and F. Lott, A study of the low frequency inertio-gravity waves observed during the Pyrinies Experiment, *J. Geophys. Res., 103,* 1747-1758, 1998.

Smyth, P., Ide, K. and M. Ghil, Multiple regimes in northern hemisphere height fields via mixture model clustering, *J. Atmos. Sci., 56,* 3704-3723, 1999.

Strong, C., Jin, F. F. and M. Ghil, Intraseasonal oscillations in a barotropic model with annual cycle, and their predictability, *J. Atmos. Sci., 52,* 2627-2642, 1995.

Thomson, D. J., Spectrum estimation and harmonic analysis, *Proc. IEEE, 70,* 1055-1096, 1982.

Thompson, D. W. and J. M. Wallace, The Arctic Oscillation signature in the wintertime geopotential height and temperature field, *Geophys. Res. Lett., 25,* 1297-1300, 1998.

Wallace, J. M. and D. S. Gutzler, Teleconnections in the geopotential height field during the Northern-Hemisphere winter, *Mon. Wea. Rev., 109,* 784-812, 1981.

Weickmann, K. M., Kiladis, G. N. and P. D. Sardeshmukh, The dynamics of intraseasonal atmospheric angular momentum oscillations, *J. Atmos. Sci., 54,* 1445-1461, 1997.

F. Lott, Laboratoire de Météorologie Dynamique du CNRS, Université Pierre et Marie Curie, 4 place Jussieu, Boite 99, 75252 Paris, France. (e-mail: flott@lmd.jussieu.fr)

M. Ghil and A. W. Robertson, Department of Atmospheric Sciences and Institute of Geophysics and Planetary Physics, University of California at Los Angeles, 405 Hilgard Avenue, Los Angeles, California 90095-1565, USA. (e-mail: ghil@atmos.ucla.edu; andy@atmos.ucla.edu)

(Received May 26, 2000; revised October 18, 2000;
accepted November 20, 2000.)